Available online at www.sciencedirect.com
ScienceDirect
Journal of Environmental Sciences 2012, 24(1) 147–151
JOURNAL OF ENVIRONMENTAL SCIENCES
ISSN 1001-0742
CN 11-2629/X
www.jesc.ac.cn

Theoretical study on the reaction mechanism of ozone addition to the double bonds of keto-limonene

Lei Jiang[1,2], Yisheng Xu[2,*], Baohui Yin[2], Zhipeng Bai[2]

1. College of Environmental Sciences and Engineering, Peking University, Beijing 100871, China
2 State Key Laboratory of Environmental Criteria and Risk Assessment, Chinese Research Academy of Environmental Sciences, Beijing 100012, China

Abstract

The reaction mechanism of ozone (O_3) addition to the double bonds of gas phase keto-limonene was investigated using *ab initio* methods. Two different possibilities for O_3 addition to the double bond were considered and two corresponding van der Waals complexes (Complex 1 and Complex 2) were found for 1-endo and 2-endo. The rate constants were calculated using the transition state theory at the CCSD(T)/6-31G(d) + CF//B3LYP/6-31G(d,p) level. The high-pressure limit of the total rate constant at 298 K was 3.51×10^{-16} cm^3/(molecule·sec), which was in a good agreement with the experimental data.

Key words: keto-limonene; O_3; transition state theory

DOI: 10.1016/S1001-0742(11)60738-9

Introduction

Limonene (4-isopropenyl-1-methyl-cyclohexene) is the most abundant monoterpene, and possesses both endocyclic and exocyclic double bonds (Guenther et al., 2000; Ramírez-Ramírez and Nebot-Gil, 2005). It is important for secondary organic aerosol (SOA) formation due to its high reactivity, and is recognized as an important precursor of tropospheric ozone formation and an essential source of OH radicals (Aschmann et al., 2002; Rickard et al., 1999). Keto-limonene (4-acetyl-1-methyl-cyclohexene, AMCH), is an important limonene oxidation product with high reactivity. It also has been found in experimental studies on the reactions of limonene with OH and NO_3 radicals and reaction of stabilized criegee intermediates from ozonolysis of limonene with H_2O (Leungsakul et al., 2005a, 2005b; Spittler et al., 2006). The initial reaction of ozone with keto-limonene forms the primary ozonide, a five-membered ring from O_3 addition to the endocyclic double bond. The primary ozonide subsequently undergoes unimolecular decomposition to yield excited Criegee intermediates or carbonyl oxide. Then, the excited Criegee intermediates are stabilized via collision to the stabilized Criegee intermediate, which reacts with various atmospheric compounds (Ryzhkov and Ariya, 2003; Criegee, 1975; Neeb et al., 1995; Hatakeyama et al., 1981), such as H_2O, SO_2 and H_2SO_4. Hence, the reaction of ozone with keto-limonene is an important oxidation process in the troposphere, and it is therefore important to clarify the oxidation mechanism for the limonene-ozone reaction system. Reactions between keto-limonene and ozone, such as SOA production from ozonolysis of keto-limonene, have been reported in previous studies (Grosjean et al., 1992; Calogirou et al., 1999; Donahue et al, 2007), and laboratory studies on the rate constant of keto-limonene reactions with O_3 (Grimsrud et al., 1975). However, important processes such as the formation of the primary ozonides, isomer-specific reactions and branch ratios are yet to be studied and the chemical natures of the aforementioned processes are yet to be understood.

In this study, two possibilities for the initial step of O_3 addition to keto-limonene were investigated using theoretical methods *ab initio* and Density Functional Theory (DFT) were employed to obtain the geometries, energies of the transition states and primary ozonides in the subsequent process of formation. Reaction and activation energies, enthalpies, and free energies for the reaction between keto-limonene and O_3 were obtained at different theory levels including CCSD(T)/6-31G(d) + CF. We also performed transition state theory (TST) calculations of the isomer-specific rate constants and branching ratios of the O_3-keto-limonene adduct isomers at the high-pressure limit.

1 Theoretical methods

Theoretical computations were carried out with the SGI ALTIX 4700 supercomputer using GAUSSIAN 03 suite of programs (Frisch et al., 2004). The geometric optimizations of all reactants, transition states, and primary ozonides were performed at B3LYP/6-31G(d,p) with harmonic vibrational frequencies analysis. The stationary points were classified as minima when no imaginary

* Corresponding author. E-mail: xuys@craes.org.cn

frequencies were found, and as a transition state if only one imaginary frequency was obtained. The DFT structures were then used in the single-point energy *Ab initio* calculations using frozen core second-order Møller-Plesset perturbation theory (MP2) and coupled-cluster theory with single and double excitations including perturbative corrections for the triple excitations (CCSD(T)), with various basis sets (Zhang et al., 2008). For more accurate single-point energy, the basis set effects on calculated energies for the O_3 keto-limonene reactions were corrected at the MP2 level, which have been recently employed for studying the complex reaction mechanisms and pathways of volatile organic compounds (VOCs) in the atmosphere (Lei et al., 2000). A correction factor (CF) was determined from the energy difference between the MP2/6-31G(d) and MP2/6-311++G(d,p) levels. Energies calculated at the CCSD(T)/6-31G(d) level were corrected using the aforementioned MP2 level corrections. This method has been validated in several studies of isoprene and limonene reactions initiated by NO_3, OH and O_3 (Lei et al., 2000; Suh et al, 2001; Zhang and Zhang, 2002; Jiang et al., 2009, 2010).

In addition, conventional transition-state theory (TST) (Wigner, 1937) was used to compute the rate constants using the optimized geometries, energies and Hessian or frequencies information for all the reactants, transition states, and primary ozonides. The reaction rate calculations were performed using the Polyrate 9.7 suite of programs (Corchado et al., 2007).

2 Results and discussion

2.1 Reaction mechanism

Figure 1 presents the optimized geometries of the stationary points for O_3 addition to keto-limonene obtained at the B3LYP/6-31G(d,p) level and the values of the most important geometrical properties.

Two transition states (TS1 and TS2) associated with the addition of O_3 to keto-limonene leading to the formation of the primary ozonides were identified. The transition-state structures were verified using frequency calculations. Each transition state had only one imaginary harmonic vibrational frequency, which was identified as the first-order saddle point. The values of imaginary frequencies for TS1 and TS2 transition states were 141i and 150i, respectively.

In the more favorable 1-endo pathway, the reaction firstly formed the van der Waals complex (Complex 1). The Complex 1 then evolved via the transition state (TS1) into a primary ozonide (PO1). As seen from Fig. 1, the CC double bond distance (1.339 Å) increased by 0.019 Å, 0.041 Å and 0.211 Å in Complex 1 (1.358 Å), TS1 (1.380 Å) and PO1 (1.550 Å) respectively, which became a single bond when the primary ozonide was forming. The disappearance of the double bond was also shown in the reaction procedure by the change in bond length The O_3-keto-limonene distances (C–O lengths) for two forming bonds of five-member ring increased to 2.681 and 2.738 Å in Complex1, but decreased to 2.321 and 2.368 Å in TS1, and to 1.444 and 1.426 Å in informed primary ozonide isomer (PO1), respectively. Another pathway of transition state (TS2) and primary ozonide (PO2) followed the same trends as those for the 1-endo pathway. We concluded that this reaction mechanism was very similar to that of O_3-limonene reaction (Jiang et al., 2010).

In comparison with the O_3-limonene reaction (Jiang et al., 2010), we found two van der Waals complexes (Complex 1 and Complex 2) prior to the corresponding transition states (TS1 and TS2) for two pathways (1-endo and 2-endo) in the O_3-keto-limonene reaction, respectively. The geometries of the optimized van der Waals structures are shown in Fig. 1. The lengths of the C–O in Complex 1 and Complex 2 were substantially longer than the C–O lengths in TS1 and TS2 due to the long-range interactions

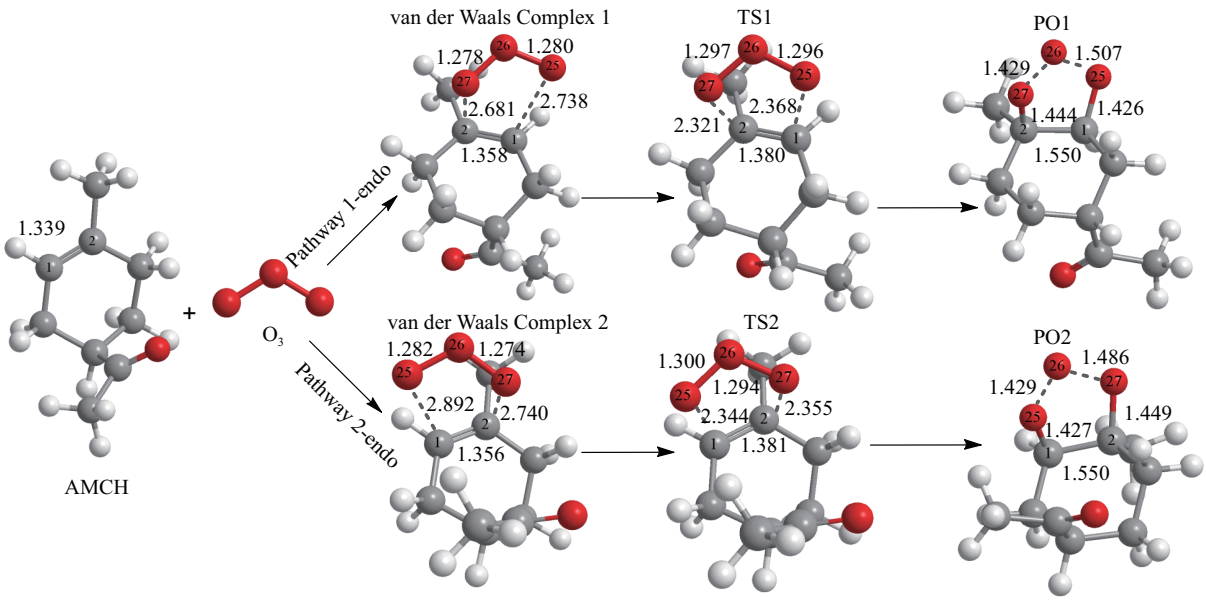

Fig. 1 Geometries of stationary points involved in the O_3 addition to keto-limonene obtained at B3LYP/6-31G(d,p) theory level. Bond distances are given in Å. TS1 and TS2 are abbreviations for 1-endo and 2-endo transition states, PO means primary ozonide.

between the reactant molecules. The two outer O atoms of the O_3 group were oriented towards the corresponding C–C double bond in both cases.

2.2 Thermochemical analysis

The O_3-keto-limonene reaction energies for two pathways computed at different theory levels with the zero-point correction are presented in Table 1. The reaction energies of the O_3 addition to keto-limonene calculated at different levels of theory were different. The values predicted by B3LYP/6-31G(d,p) and CCSD(T)/6-31G(d) were close, within 1.79 kcal/mol, and were lower than those obtained using MP2. The MP2 values obtained using different basis sets differed by –5.21 and –5.57 kcal/mol. The values obtained at CCSD(T)/6-31G(d) level theory were 7.35–12.94 kcal/mol more stable than those calculated with MP2. At the CCSD(T)/6-31G(d) + CF theory level, the primary ozonides were –53.61 and –53.87 kcal/mol more stable than the separate O_3 and keto-limonene. In addition, PO1 was slightly more stable than PO2 by 0.26 kcal/mol.

As seen from Table 1, the activation energies of the O_3 addition reaction computed at all theory levels with zero-point correction included were negative, which corresponded to unreliable barriers for the O_3 addition to ethylene isoprene and limonene reactions reported in previous studies (Zhang and Zhang, 2002; Jiang et al., 2010). The negative activation energies implied that cycloaddition of O_3 to keto-limonene occurred through a van der Waals complex prior to the transition state (Zhang and Zhang, 2002; Olzmann et al., 1997). This was confirmed by the appearance of Complex 1 and Complex 2. The negative activation energies given by MP2 with two different basis sets were very similar, with differences of 0.25 and 0.76 kcal/mol, and corresponding activation energies were lower than B3LYP/6-31G(d,p) and CCSD(T)/6-31G(d) within the limits of 7.44 and 10.07 kcal/mol, respectively. The activation energies obtained at the CCSD(T)/6-31G(d) + CF theory level were –0.61 kcal/mol for 1-endo and –0.59 kcal/ mol for 2-endo. Figure 2 illustrates the relative energies of the stationary points located on the singlet ground-state separate O_3 and keto-limonene potential energy surface at the CCSD(T)/6-31G(d) + CF theory level.

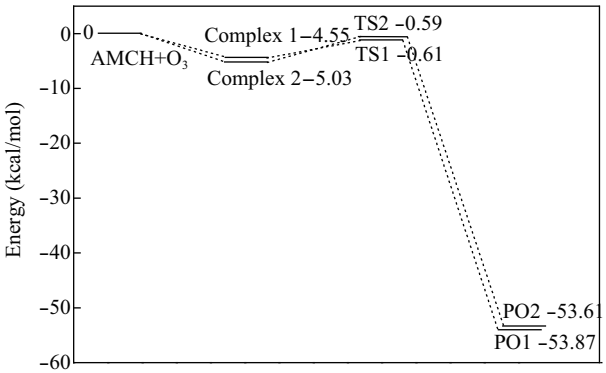

Fig. 2 O_3-keto-limonene reaction coordinates: relative energies of the stationary points located on the separate O_3 and keto-limonene ground-state potential energy surface. The energy values are calculated using CCSD(T)/6-31G(d) +CF//B3LYP/6-31G(d,p).

Reaction and activation enthalpies for the reaction between keto-limonene and O_3 obtained at different theory levels with thermal correction to enthalpy included are also listed in Table 1. The reaction and activation enthalpies values were in accordance with those of reaction and activation energies. At the CCSD(T)/6-31G(d) + CF level, the reactions between keto-limonene and O_3 were exothermic by 55.09 and 54.95 kcal/mol, while the computed activation enthalpies were –1.24 and –1.41 kcal/mol.

Reaction and activation Gibbs free energies with thermal correction for the reaction between keto-limonene and O_3 computed at different theory levels are shown in Table 1. The reaction and activation Gibbs free energy values were in accordance with those of reaction and activation energies. At the CCSD(T)/6-31G(d) + CF theory level, the reaction Gibbs free energies of the reaction between keto-limonene and O_3 were between –40.04 and –39.43 kcal/mol. The strong negativity of the Gibbs free energy changes indicated that the O_3-keto-limonene reaction was spontaneous.

Relative energies including the zero-point energy (ZPE) correction for Complex 1 and Complex 2 with respect to

Table 1 O_3-keto-limonene reaction energy, activation enthalpies and Gibbs free energy computed at different theory levels for the two pathways[a] (unit: kcal/mol)

Method	MP2/6-31G(d,p)	MP2/6-311++G(d,p)	B3LYP/6-31G(d,p)	CCSD(T)/6-31G(d)	CCSD(T)/6-31G(d)+CF
$RE_{1\text{-endo}}$	–52.08	–46.51	–57.66	–59.45	–53.87
$RE_{2\text{-endo}}$	–51.47	–46.26	–57.40	–58.82	–53.61
$\Delta E_{1\text{-endo}}$	–10.64	–10.39	–3.92	–0.87	–0.61
$\Delta E_{2\text{-endo}}$	–11.42	–10.66	–3.98	–1.35	–0.59
$RH_{1\text{-endo}}$	–53.30	–47.72	–58.87	–60.66	–55.09
$RH_{2\text{-endo}}$	–52.81	–47.59	–58.73	–60.16	–54.95
$\Delta H_{1\text{-endo}}$	–11.27	–11.02	–4.55	–1.50	–1.24
$\Delta H_{2\text{-endo}}$	–12.23	–11.48	–4.80	–2.17	–1.41
$RG_{1\text{-endo}}$	–38.25	–32.68	–43.83	–45.62	–40.04
$RG_{2\text{-endo}}$	–37.29	–32.08	–43.22	–44.64	–39.43
$\Delta G_{1\text{-endo}}$	2.18	2.43	8.90	11.95	12.21
$\Delta G_{2\text{-endo}}$	2.20	2.96	9.64	12.27	13.03

[a] Optimized geometries, vibrational frequencies, ZPE, thermal correction to enthalpy and thermal correction to Gibbs free energy obtained at the B3LYP/6-31G(d,p) level.

RE and ΔE: reaction and activation energies with zero-point correction;

RH and ΔH: reaction and activation enthalpies with thermal correction;

RG and ΔG: reaction and activation Gibbs free energies with thermal correction.

Table 2 Relative energies of Complex 1 and Complex 2 in respect to reactants with zero-point correction included computed at different theory levels for the two pathways (1-endo and 2-endo)[a] (unit: kcal/mol)

Method	MP2/ 6-31G(d)	MP2/ 6-311++G(d,p)	B3LYP/6-31G(d,p)	CCSD(T)/6-31G(d)	CCSD(T)/6-31G(d)+CF
$\Delta E_{vdw,1\text{-endo}}$	–8.58	–9.33	–4.70	–3.80	–4.55
$\Delta E_{vdw,2\text{-endo}}$	–8.87	–9.08	–4.97	–4.28	–5.03

[a] Optimized geometries, vibrational frequencies and ZPE obtained at the B3LYP/6-31G(d,p) level.

reactants computed at different theory levels with different basis sets are given in Table 2. The CCSD(T)/6-31G(d) + CF values for Complex 1 and Complex 2 were –4.55 kcal/mol and –5.03 kcal/mol, which were lower than those of the corresponding TS (–0.61 and –0.59 kcal/mol). This indicated that a possible associated van der Waals complex was formed before the transition state. This was also similar to that of the O_3-limonene reaction (Jiang et al., 2010). Van der Waals complexes can be observed in most quantum mechanical representations of reaction profiles, but they are normally ignored as they do not have a profound effect on kinetics (Alvarez-Idaboy et al., 2000) and are not chemically relevant in the reaction mechanisms (García-Cruz et al., 1999).

2.3 Rate constant calculations

The results for the TST high-pressure limit rate constants at 298 K using the CCSD(T)/6-31G(d) + CF//B3LYP/6-31G(d,p) theory level for O_3 addition to keto-limonene are shown in Table 3. For O_3-keto-limonene reaction, the total rate constant was 3.51×10^{-16} cm^3/(molecule·sec), which was consistent with the experimental value (1.5×10^{-16} cm^3/(molecule·sec)). The rate constants of the two pathways were 2.8×10^{16} and 7.1×10^{17} cm^3/(molecule·sec), respectively and the relative branching was 0.8:0.2 for 1-endo : 2-endo pathways. The rate of 1-endo pathway was about four times faster than that of 2-endo. The difference in the reaction rates was attributed to the steric hindrance effect. As shown in Fig. 1, the acetyl and methyl groups in TS2 were much closer to the double bond of the reaction position than those in TS1.

Due to the fact that limonene emissions in the troposphere have been observed in summer and winter and keto-limonene is an important limonene oxidation product, the rate constants in the temperature range 257–310 K were computed. The corresponding data are also collected in Table 4. For the reaction of keto-limonene with O_3 it can be seen that the rate constants in the temperature range of 257–310 K were between 3.77×10^{-16} and 3.55×10^{-16} cm^3/(molecule·sec), implying that the rate constant correlated negatively with temperature dependence. But the changes between the rate constants of different temperature were very small, within $0.22\times10^{-16}cm^3$/(molecule·sec) as the largest difference from 257 to 310 K.

Table 3 Calculated transition-state theory high-pressure limit rate constants and branching ratios for the formation of O_3-keto-limonene reactions[a]

Reaction	Rate of formation (cm^3/(molecule·sec))	Branching ratio	Reference
1-endo	2.8×10^{-16}	0.8	1.5×10^{-16}[b]
2-endo	7.1×10^{-17}	0.2	
Total	3.51×10^{-16}	1.0	

[a] Calculated at the CCSD(T)/6-31G(d) + CF // B3LYP/6-31G(d,p) level of theory; [b] Atkinson and Aschmann, 1993.

Table 4 Calculated TST high-pressure limit rate constants for the formation of O_3-keto-limonene reactions at different temperatures[a]

Species	Rate of formation (cm^3/(molecule·sec))	Temperature (K)
Keto-limonene + O_3	3.77×10^{-16}	257
	3.65×10^{-16}	273
	3.62×10^{-16}	280
	3.59×10^{-16}	288
	3.57×10^{-16}	300
	3.55×10^{-16}	310

[a] Calculated at the CCSD(T)/6-31G(d) + CF/B3LYP/6-31G(d,p) level of theory.

3 Conclusions

In this study, the initial O_3 addition to keto-limonene was investigated using quantum chemical methods. Our results indicated that the 1-endo pathway was more favorable branching for the initial O_3-keto-limonene reaction step. The calculated rate constant at 298 K using CCSD(T)/6-31G(d) + CF was 3.51×10^{16} cm^3/(molecule·sec) for keto-limonene, in good agreement with the experimental studies, and the rate constants of the two reaction channels were 2.8×10^{-16} and 7.1×10^{-17} cm^3/(molecule·sec) for 1-endo and 2-endo, respectively. Temperature dependence with rate constants was very small within 0.22×10^{-16} cm^3/(molecule·sec).

Acknowledgments

This work was supported by the National Natural Science Foundation of China (No. 40975073). Authors thank the CRAES Supercomputing Facilities (SGI 4700 super computers) for providing computational resources. Special thanks to Du Jian, Wang Bo, Zhang Zeyan, and Zeng Rui for assisting with the maintenance of the quantum chemical calculations.

References

Alvarez-Idaboy J R, Mora-Díez N, Vivier-Bunge A, 2000. A quantum chemical and classical transition state theory explanation of negative activation energies in oh addition to substituted ethenes. *Journal of the American Chemical Society*, 122(15): 3715–3720.

Aschmann S M, Arey J, Atkinson R, 2002. OH radical formation from the gas-phase reactions of O_3 with a series of terpenes. *Atmospheric Environment*, 36(27): 4347–4355.

Atkinson R, Aschmann S M, 1993. Hydroxyl radical production from the gas-phase reactions of O_3 with a series of alkenes

under atmospheric conditions. *Environmental Science & Technology*, 27(7): 1357–1363.

Calogirou A, Larsen B R, Kotzias D, 1999. Gas-phase terpene oxidation products: A review. *Atmospheric Environment*, 33(9): 1423–1439.

Corchado J C, Chuang Y Y, Fast P L, Hu W P, Liu Y P, Lynch G C et al., 2007. POLYRATE Version 9.7. University of Minnesota Minneapolis.

Criegee R, 1975. Mechanism of ozonolysis. *Angewandte Chemie International Edition*, 14(11): 745–751.

Donahue N M, Tischuk J E, Marquis B J, Huff Hartz K E, 2007. Secondary organic aerosol from limona ketone: Insights into terpene ozonolysis via synthesis of key intermediates. *Physical Chemistry Chemical Physics*, 9(23): 2991–2998.

Frisch M J, Trucks G W, Schlegel H B, Schlegel H B, Scuseria G E, Robb M A et al., 2004. Gaussian 03, Revision E.01 Gaussian, Wallingford, CT.

García-Cruz I, Ruiz-Santoyo M E, Alvarez-Idaboy J R, Vivier-Bunge A, 1999. *Ab-initio* study of initial atmospheric oxidation reactions of C_3 and C_4 alkanes. *Journal of Computational Chemistry*, 20(8): 845–856.

Grimsrud E P, Westberg H H, Rasmussen R A, 1975. Atmospheric reactivity of monoterpene hydrocarbons, NO_x photooxidation and ozonolysis. *International Journal of Chemical Kinetics*, 7(1): 183–195.

Grosjean D, Williams E L, Seinfeld J H, 1992. Atmospheric oxidation of selected terpenes and related carbonyls: Gas-phase carbonyl products. *Environmental Science & Technology*, 26(8): 1526–1533.

Guenther A, Geron C, Pierce T, Lamb B, Harley P, Fall R, 2000. Natural emissions of non-methane volatile organic compounds, carbon monoxide, and oxides of nitrogen from North America. *Atmospheric Environment*, 34(12-14): 2205–2230.

Hatakeyama S, Bandow H, Okuda M, Akimoto H, 1981. Reactions of peroxymethylene and methylene (1A1) with water in the gas phase. *The Journal of Physical Chemistry*, 85(15): 2249–2254.

Jiang L, Wang W, Xu Y S, 2009. Theoretical investigation of the NO_3 radical addition to double bonds of limonene. *International Journal of Molecular Sciences*, 10(9): 3743–3754.

Jiang L, Wang W, Xu Y S, 2010. *Ab Initio* investigation of O_3 addition to double bonds of limonene. *Chemical Physics*, 368(3): 108–112.

Lei W F, Derecskei-Kovacs A, Zhang R Y, 2000. *Ab Initio* study of OH addition reaction to isoprene. *Journal of Chemical Physics*, 113(13): 5354–5360.

Leungsakul S, Jaoui M, Kamens R M, 2005a. Kinetic mechanism for predicting secondary organic aerosol formation from the reaction of *d*-limonene with ozone. *Environmental Science & Technology*, 39(24): 9583–9594.

Leungsakul S, Jeffries H E, Kamens R M, 2005b. A kinetic mechanism for predicting secondary aerosol formation from the reactions of *d*-limonene in the presence of oxides of nitrogen and natural sunlight. *Atmospheric Environment*, 39(37): 7063–7082.

Neeb P, Horie O, Moortgat G K, 1995. The nature of the transitory product in the gas-phase ozonolysis of ethene. *Chemical Physics Letters*, 246(1-2): 150–156.

Olzmann M, Kraka E, Cremer D, Gutbrod R, Andersson S, 1997. Energetics, kinetics, and product distributions of the reactions of ozone with ethene and 2,3-dimethyl-2-butene. *The Journal of Physical Chemistry A*, 101(49): 9421–9429.

Ramírez-Ramírez V M, Nebot-Gil I, 2005. Theoretical study of the OH addition to the endocyclic and exocyclic double bonds of the *d*-limonene. *Chemical Physics Letters*, 409(1-3): 23–28.

Rickard A R, Johnson D, McGill C D, Marston G, 1999. OH yields in the gas-phase reactions of ozone with alkenes. *The Journal of Physical Chemistry A*, 103(38): 7656–7664.

Ryzhkov A B, Ariya P A, 2003. A theoretical study of the reactions of carbonyl oxide with water in atmosphere: The role of water dimer. *Chemical Physics Letters*, 367(3-4): 423–429.

Spittler M, Barnes I, Bejan I, Brockmann K J, Benter Th, Wirtz K, 2006. Reactions of NO_3 radicals with limonene and α-pinene: Product and SOA formation. *Atmospheric Environment*, 40(Suppl.): 116–127

Suh I, Lei W F, Zhang R Y, 2001. Experimental and theoretical studies of isoprene reaction with NO_3. *The Journal of Physical Chemistry A*, 105(26): 6471–6478.

Wigner E, 1937. Calculation of the rate of elementary association reactions. *The Journal of Chemical Physics*, 5(9): 720–725.

Zhang D, Zhang R Y, 2002. Mechanism of OH formation from ozonolysis of isoprene: A quantum-chemical study. *Journal of the American Chemical Society*, 124(11): 2692–2703.

Zhang Q Z, Li S Q, Qu X H, Shi X Y, Wang W X, 2008. A quantum mechanical study on the formation of PCDD/Fs from 2-Chlorophenol as precursor. *Environmental Science & Technology*, 42(19): 7301–7308.